processes

Article

# Boosting $CO_2$ Uptake from Waste Concrete Powder Using Artificial Intelligence and the Marine Predators Algorithm

**Hegazy Rezk [1], Ali Alahmer [2,3,*], Rania M. Ghoniem [4] and Samer As'ad [5]**

[1] Department of Electrical Engineering, College of Engineering in Wadi Alddawasir, Prince Sattam bin Abdulaziz University, Al-Kharj 11942, Saudi Arabia; hr.hussien@psau.edu.sa
[2] Department of Mechanical Engineering, Tuskegee University, Tuskegee, AL 36088, USA
[3] Department of Mechanical Engineering, Faculty of Engineering, Tafila Technical University, Tafila 66110, Jordan
[4] Department of Information Technology, College of Computer and Information Sciences, Princess Nourah bint Abdulrahman University, Riyadh 11671, Saudi Arabia; rmghoniem@pnu.edu.sa
[5] Renewable Energy Engineering Department, Faculty of Engineering, Middle East University, Amman 11831, Jordan; sasad@meu.edu.jo
* Correspondence: aza0300@auburn.edu or a.alahmer@ttu.edu.jo

**Abstract:** Waste concrete powder (WCP) is emerging as a potential method of adoption for $CO_2$ sequestration due to its ability to chemically react with carbon dioxide and trap it within its structure. This study explores the application of artificial intelligence (AI) and the Marine Predators Algorithm (MPA) to maximize the absorption of $CO_2$ from waste concrete powder generated by recycling plants for building and demolition debris. Initially, a model is developed to assess $CO_2$ uptake according to carbonation time (CT) and water-to-solid ratio (WSR), utilizing the adaptive neuro-fuzzy inference system (ANFIS) modeling approach. Subsequently, the MPA is employed to estimate the optimal values for CT and WSR, thereby maximizing $CO_2$ uptake. A significant improvement in modeling accuracy is evident when the ANOVA method is replaced with ANFIS, leading to a substantial increase of approximately 19% in the coefficient of determination (R-squared) from 0.84, obtained through ANOVA, to an impressive 0.9999 obtained through the implementation of ANFIS; furthermore, the utilization of ANFIS yields a substantial reduction in the root mean square error (RMSE) from 1.96, as indicated by ANOVA, to an impressively low value of 0.0102 with ANFIS. The integration of ANFIS and MPA demonstrates impressive results, with a nearly 30% increase in the percentage value of $CO_2$ uptake. The highest $CO_2$ uptake of 3.86% was achieved when the carbonation time was 54.3 h, and the water-to-solid ratio was 0.27. This study highlights the potential of AI and the MPA as effective tools for optimizing $CO_2$ absorption from waste concrete powder, contributing to sustainable waste management practices in the construction industry.

**Keywords:** waste concrete powder; $CO_2$ uptake; marine predators algorithm; ANFIS modeling; mineral carbonation



**Citation:** Rezk, H.; Alahmer, A.; Ghoniem, R.M.; As'ad, S. Boosting $CO_2$ Uptake from Waste Concrete Powder Using Artificial Intelligence and the Marine Predators Algorithm. *Processes* **2023**, *11*, 2655. https://doi.org/10.3390/pr11092655

Academic Editors: Paola Ammendola, Haris Ishaq and Liwei Zhang

Received: 30 July 2023
Revised: 18 August 2023
Accepted: 30 August 2023
Published: 5 September 2023



## 1. Introduction

Currently, the optimization of $CO_2$ uptake has become a crucial focus in the pursuit of sustainable solutions to mitigate climate change. The atmospheric $CO_2$ concentration has been rapidly increasing at an exceptional rate of 2.2 ppm/year [1]. It is estimated that by approximately 2050, the atmospheric $CO_2$ concentration may reach around 450 ppm. Consequently, this increase in $CO_2$ levels is projected to cause a temperature rise of 2 °C to 3 °C on the Earth's surface due to the greenhouse effect [2]. To tackle these challenges, numerous methods and techniques have been developed to capture and store $CO_2$, each offering its own advantages and potential applications [3–5]. Carbon capture and storage is a method that captures $CO_2$ emissions generated from industrial processes and securely stores them underground, ensuring that they do not escape into the atmosphere [6,7].

Carbon capture and utilization refers to the process of capturing $CO_2$ emissions and converting them into valuable commodities, such as chemicals, plastics, or fuels [8,9]. Biological carbon sequestration exploits the natural capacity of plants and trees to absorb $CO_2$ through photosynthesis [10]. Enhanced weathering accelerates natural processes to capture $CO_2$ by applying crushed minerals like basalt or olivine, which react with $CO_2$ to form stable carbonates [11]. Direct air capture uses specialized technologies to extract $CO_2$ directly from the ambient air [12]. The choice of approach relies on various factors, including the $CO_2$ emission source, implementation scale, economic feasibility, and environmental considerations.

The continuous growth of the construction industry has led to a rise in waste generation, particularly in the form of concrete by-products. Traditionally, waste concrete powder has been viewed as an environmental concern, typically leading to landfill disposal or pollution if not handled properly [13]. In the European Union, construction and demolition waste comprise approximately 35–46% of the total waste stream in the European Union [14]. Notably, end-of-life concrete makes up a significant portion of this construction and demolition waste, contributing around 12–40% to the overall waste volume [15]; however, recent studies highlighted the potential of waste concrete powder as a valuable resource for $CO_2$ sequestration [16]. By utilizing waste concrete powder in a controlled environment, we can enhance its ability to capture and store $CO_2$, turning it into a beneficial asset rather than a liability [17]. Studies have specifically explored the recycling of alkaline-rich waste, including filter-pressed concrete slurry waste, through accelerated carbonation techniques [18,19].

Waste concrete powder (WCP) exhibits promising potential as an option for carbon dioxide ($CO_2$) sequestration, owing to its capability to undergo chemical reactions with $CO_2$ and effectively store it within its structure. The $CO_2$ uptake capacity refers to the amount of carbon dioxide that can be absorbed and stored by WCP through a process known as mineral carbonation [20]. Mineral carbonation is a process that converts $CO_2$ into solid mineral forms, thereby effectively sequestering the carbon and preventing its release into the atmosphere [21]. The $CO_2$ uptake capacity of WCP is influenced by various factors such as the carbonation time (CT) (duration of the carbonation process) and the water-to-solid ratio (WSR), which evaluates the amount of water used in relation to the quantity of WCP [22]. Optimizing these variables is crucial for enhancing the $CO_2$ uptake capacity of WCP and establishing it as a sustainable solution for carbon capture. This entails selecting the appropriate WCP composition, identifying optimal $CO_2$ absorption conditions, and developing efficient implementation techniques [23]. Studies have shown that the ability of WCP to absorb $CO_2$ can be significantly enhanced by optimizing these factors [24]. For example, enhancing the fineness of the crushed concrete particles, which refers to reducing the particle size of WCP, can create more surface area for the chemical reaction to occur, leading to a higher $CO_2$ uptake capacity [25]. Kaliyavaradhan et al. [26] explored the dual functionality of concrete slurry waste as a $CO_2$ capture agent and a supplementary cementitious material. The study investigated the influence of WSR and reaction time on the $CO_2$ uptake capacity of concrete slurry waste using response surface methodology (RSM). The optimal conditions were found to be a w/s ratio of 0.25 and a reaction time of 72 h, resulting in a remarkable maximum $CO_2$ uptake of 20.4%.

Accelerated mineral carbonation has gained considerable attention as a promising technique in carbon capture and storage. This process allows for the long-term storage of $CO_2$ by employing a controlled chemical reaction between $CO_2$ and alkaline oxides, like calcium oxide (CaO) and magnesium oxide (MgO), commonly present in natural silicate rocks or industrial by-products. The outcome of this reaction is the formation of stable carbonate compounds, such as calcium carbonate ($CaCO_3$) and magnesium carbonate ($MgCO_3$), which find diverse practical applications. Pan et al. [27] estimated the global $CO_2$ mitigation potential of applying accelerated carbonation to various alkaline solid wastes. The results indicate that $CO_2$ mineralization and utilization can significantly reduce $CO_2$ emissions, achieving a 12.5% global reduction equivalent to 4.02 Gt per year.

A significant number of experimental investigations are dedicated to evaluating and optimizing $CO_2$ storage through accelerated carbonation processes. These studies aim to optimize operational parameters, encompassing temperature, pressure, gas humidity, liquid and gas flow rates, liquid-to-solid ratio, solid pre-treatment, and particle size [28–30]. Based on experimental results, the filter-pressed concrete slurry waste has exhibited an impressive $CO_2$ sequestration capacity, reaching up to 75% of the total $CO_2$ uptake in just a few hours. Over a duration of 144 h of carbonation, concrete slurry waste demonstrated the capability to capture 110 g of $CO_2$/kg of dry concrete slurry waste [31].

Due to the costly, limited, and time-intensive nature of conducting experimental studies on $CO_2$ uptake from waste concrete powder across different operational conditions to determine the highest $CO_2$ uptake, there is a need for alternative effective approaches to assess characteristics effectively. Employing optimization methods offers an advantageous approach to minimize the necessity for extensive experimental trials [32–34]. This study aims to bridge the existing gap in the application of AI techniques and the recent optimization method, specifically the Marine Predators Algorithm (MPA), for maximizing $CO_2$ absorption from WCP. Although WCP has shown promise as a potential $CO_2$ sequestration agent, there is a lack of comprehensive studies that explore the optimization of $CO_2$ uptake from WCP using advanced AI algorithms. Therefore, this study aims to bridge this gap by integrating the ANFIS modeling approach and the MPA to identify optimal values for CT and WSR, thus, enhancing $CO_2$ absorption from WCP. The primary point of this research is to enhance $CO_2$ uptake through the utilization of the MPA in combination with ANFIS modeling. The initial step involves the development of an ANFIS model based on experimental datasets to simulate the $CO_2$ uptake, considering the CT and WST as variables. Subsequently, the MPA is employed to identify the optimal values for the CT and WSR, aiming to maximize the $CO_2$ uptake. Furthermore, this study includes a comparative analysis between ANFIS modeling and the traditional ANOVA method in terms of accuracy and prediction capabilities for $CO_2$ uptake from WCP. This analysis provides insights into the superiority of ANFIS modeling, which exhibits a substantial increase in the R-squared and a significant reduction in the RMSE.

The contribution aspect of this study is observed in the integration of AI techniques, particularly ANFIS modeling and the MPA, to optimize $CO_2$ absorption from waste concrete powder. While previous studies have primarily focused on exploring the $CO_2$ sequestration potential of WCP, a limited number have employed advanced AI algorithms to enhance the absorption process. By utilizing ANFIS modeling, this research improves the accuracy and prediction capabilities for $CO_2$ uptake, leading to significant advancements in modeling accuracy; moreover, the integration of ANFIS and the MPA further enhances the percentage value of $CO_2$ uptake, demonstrating the effectiveness of this novel approach. The findings of this study contribute to sustainable waste management practices in the construction industry by providing valuable insights into optimizing $CO_2$ absorption from waste concrete powder using AI techniques.

The key contributions of the paper can be outlined as follows:

- Development of a robust ANFIS model for $CO_2$ uptake, considering carbonation time and water-to-solid ratio;
- Introduction of a novel implementation of MPA to enhance $CO_2$ uptake;
- Conducting a thorough analysis and comparison between the proposed Marine Predators Algorithm (MPA) and various featured algorithms such as Particle Swarm Optimization (PSO), Genetic Algorithm (GA), Harris Hawks Optimization (HHO), and Cuckoo Search (CS) to validate the efficacy of the MPA method; furthermore, employing statistical tests to ensure an equitable and objective assessment of the different metaheuristic algorithms performed.

## 2. Approach and Methodology

### *2.1. Dataset Description*

In order to enhance the absorption of $CO_2$ from waste concrete powder, an initial step involved the development of an ANFIS model. This model was designed to simulate $CO_2$ absorption by considering the CT and the WSR. To facilitate this process, a dataset with the permission of the license number 5580660002812 was utilized [23]. The experimental trials, as depicted in Table 1, encompassed a range of WSR from 0.1 to 0.7 and CT from 1 to 168 h. In total, 23 experimental runs were performed to train and validate the ANFIS model for $CO_2$ uptake analysis.

**Table 1.** Dataset description for training and testing the ANFIS model of $CO_2$ uptake.

| CT (h) | WSR | $CO_2$ Uptake (%) |
|---|---|---|
| 120 | 0.7 | 2.44 |
| 72 | 0.1 | 1.74 |
| 168 | 0.4 | 2.94 |
| 120 | 0.4 | 2.87 |
| 24 | 0.25 | 2.47 |
| 72 | 0.7 | 0.89 |
| 72 | 0.4 | 2.71 |
| 168 | 0.1 | 2.15 |
| 1 | 0.1 | 0.65 |
| 120 | 0.25 | 2.56 |
| 1 | 0.1 | 0.65 |
| 120 | 0.1 | 2.07 |
| 72 | 0.4 | 2.71 |
| 168 | 0.4 | 2.94 |
| 168 | 0.7 | 2.91 |
| 1 | 0.7 | 0.03 |
| 24 | 0.55 | 1.56 |
| 1 | 0.7 | 0.03 |
| 1 | 0.4 | 0.81 |
| 168 | 0.7 | 2.91 |
| 168 | 0.1 | 2.15 |
| 72 | 0.55 | 2.67 |
| 72 | 0.4 | 2.71 |

### *2.2. ANFIS Model of $CO_2$ Uptake*

The ANFIS, originating in the early 1990s, is a specialized form of an artificial neural network [35]. It combines the interpretability of fuzzy systems with the learning capabilities of neural networks, specifically based on the Takagi–Sugeno fuzzy inference system [36]. The fundamental principle of ANFIS revolves around mapping inputs to outputs through a sequence of fuzzy IF-THEN rules and learning algorithms. This feature enables the system to effectively handle nonlinear functions and dynamically adapt to evolving input/output data, making it well-suited for a diverse range of applications such as prediction, pattern recognition, control, and decision-making [37]. The ANFIS system is structured with three essential phases: the fuzzifier, inference engine, and defuzzifier, visually presented in Figure 1.

The initial operation in the ANFIS system involves the transformation (mapping) of crisp input values into fuzzy sets. In this phase, specific membership functions (MFs) are employed to achieve the task. These MFs are designed as convex functions, mapping the inputs to a restricted range within the interval of [0, 1]. The domain of discourse for the input can be divided into multiple MFs based on the context or application under consideration. Fuzzy membership functions (MFs) encompass various forms, including Gaussian, triangular, and trapezoidal, among others.

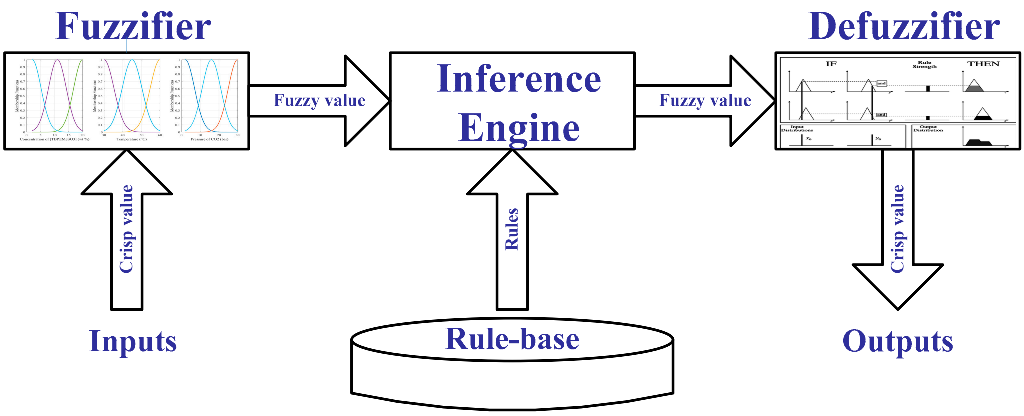


**Figure 1.** The phases of ANFIS.

The rule set consists of fuzzy criteria that dictate the relationship between the inputs and outputs of the system.

These rules, regardless of their type, follow the IF-THEN format. There are two categories of fuzzy sets available, and the selection between them depends on the specific nature of the problem. The two classifications of fuzzy rules are referred to as Mamdani and Sugeno styles. In a system with two inputs ($x$ and $y$) and one output ($f$), the rule structure is determined by the two types of fuzzy rules and can be represented as follows:

$$\text{In a Sugeno-type fuzzy rule, IF } x \text{ is } A_1 \text{ and } y \text{ is } B_1 \text{ THEN } f_1 = p_1x + q_1y + r_1 \tag{1}$$

$$\text{IF } x \text{ is } A_2 \text{ and } y \text{ is } B_1 \text{ THEN } f_2 = p_2x + q_2y + r_2 \tag{2}$$

where "$A_1$, $A_2$, $B_1$ are $B_2$ are fuzzy sets associated with premise input variables $x$ and $y$, respectively, while, $p_1$, $q_1$, $r_1$ and $p_2$, $q_2$, $r_2$ are consequent part parameters". The estimation of the final output is calculated as follows:

$$f = \tilde{\omega}_1 f_1 + \tilde{\omega}_2 f_2 \text{ (Output Layer)} \tag{3}$$

$$\text{Defuzzification Layer: Evaluating } \tilde{\omega}_1 g_1(x, y) \; and \; \tilde{\omega}_2 g_2(x, y) \tag{4}$$

$$\tilde{\omega}_1 = \frac{\omega_1}{\omega_1 + \omega_2} \text{ and } \tilde{\omega}_2 = \frac{\omega_2}{\omega_1 + \omega_2} \quad \text{(NLayer)} \tag{5}$$

$$\omega_1 = \mu_{A_1} * \mu_{B_1} \text{ and } \omega_2 = \mu_{A_2} * \mu_{B_2} \text{ ($\pi$ Layer)} \tag{6}$$

$$\text{Fuzzification Layer: } \mu_{A_1},\ \mu_{A_2}, \mu_{B_1} \text{ and } \mu_{B_2} \text{ are the MF grades of the two inputs} \tag{7}$$

The generation of fuzzy rules is typically accomplished either through system experts or by employing a clustering algorithm on the dataset. In this phase, the IF-THEN statements are triggered to deduce their corresponding outputs based on a specific set of inputs.

In particular, the implication method is employed to determine the output of each rule, providing a range of techniques for its application. Among these techniques, the Min (Intersection) operation is the most commonly employed. Once the rules are activated, the outputs of all rules are combined or aggregated to yield a single output value. In the case of Mamdani-criterion fuzzy rules, in cases where the rule's output is represented as a fuzzy value, the Max (Union) operation is utilized to determine the final outcome. Conversely, for Sugeno-criterion fuzzy rules, the final output is obtained by utilizing a weighted average.

## 2.3. Parameter Identification: Marine Predators Algorithm (MPA)

The MPA is an innovative metaheuristic search technique, inspired by the optimal foraging behavior and encounter rate policies exhibited by marine creatures in nature [38]. The MPA emulates the foraging strategies used by marine creatures in their pursuit of food through a three-phase approach [39]. Phase one is implemented during the initial third of the total iterations $t_{Max}$, and its modeling can be expressed as follows:

$$\begin{aligned} D_i &= R_B \otimes (Elite_i - R_B \otimes Pre\ y_i) \\ Pre\ y_{i+1} &= Pre\ y_i + 0.5 \cdot R \otimes D_i \end{aligned} \tag{8}$$

where $D_i$ denotes the step size of the ith predator; $R_B$ is a vector generated based on the distribution of Brownian motion; R represents random numbers within the range [0, 1]; and the symbol $\otimes$ denotes entry-wise multiplications. When the iteration t falls within the second third of $t_{Max}$, phase two is initiated, which is further divided into two subphases. If $t$ is less than half of $t_{Max}$, phase two can be mathematically expressed as follows:

$$\begin{aligned} D_i &= R_L \otimes (Elite_i - R_L \otimes Pre\ y_i) \\ Pre\ y_{i+1} &= Pre\ y_i + 0.5 \cdot R \otimes D_i \end{aligned} \tag{9}$$

where $R_L$ represents a vector generated using the distribution of Lévy motion. If the iteration $t$ is greater than half of $t_{Max}$, phase 2 can be mathematically expressed as follows:

$$\begin{aligned} D_i &= R_B \otimes (R_B \otimes Elite_i - Pre\ y_i) \\ Pre\ y_{i+1} &= Elite_i + 0.5 \cdot CF \otimes D_i \\ CF &= [1 - \left(\frac{t}{t_{Max}}\right)]^{2t/t_{Max}} \end{aligned} \tag{10}$$

The final phase can be represented by the following equation:

$$\begin{aligned} D_i &= R_L \otimes (R_L \otimes Elite_i - Pre\ y_i) \\ Pre\ y_{i+1} &= Elite_i + 0.5 \cdot CF \otimes D_i \end{aligned} \tag{11}$$

Figure 2 illustrates the flowchart of the MPA algorithm.

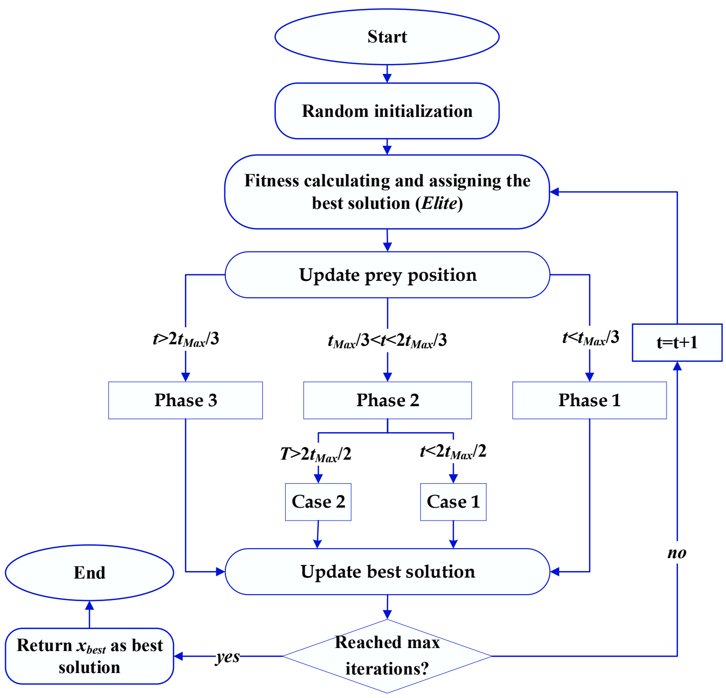


**Figure 2.** The flowchart of the MPA.

The objective of the optimization phase is to acquire the optimal values of CT and WSR. In the MPA optimization process, these variables are treated as decision variables, while $CO_2$ uptake serves as the objective function to be maximized. The problem can be expressed as:

$$x = \underset{x \in R}{\operatorname{argmax}}(y) \tag{12}$$

where $x$ denotes the set of input variables, and y represents the output variable.

## 3. Results and Discussion

This study examined the $CO_2$ absorption from WCP, with a focus on assessing the impacts of two critical factors: carbonation time (CT) and water-to-solid ratio (WSR). The investigation harnessed the power of artificial intelligence (AI) and the Marine Predators Algorithm (MPA) to pinpoint optimal values for these parameters.

The impact of carbonation time (CT) on $CO_2$ uptake from waste concrete powder is a pivotal aspect in assessing the carbon capture potential of this material. Carbonation time refers to the duration of exposure of waste concrete powder to $CO_2$-rich environments, initiating chemical reactions between $CO_2$ and the calcium-containing compounds within the concrete. According to Table 1, longer CTs are associated with several notable effects on $CO_2$ uptake. With an increase in the CT, there is a tendency for enhanced $CO_2$ uptake driven due to enhanced penetration, leading to more extensive chemical reactions and calcium carbonate formation; however, identifying the optimal carbonation duration becomes crucial, as beyond a certain point, additional $CO_2$ exposure might yield diminishing returns in $CO_2$ absorption. Moreover, prolonged carbonation can induce physical changes in waste concrete powder, influencing properties like porosity, density, and strength, which impact its applicability.

Exploring the impact of the water-to-solid ratio (WSR) on $CO_2$ uptake from WCP constitutes a vital aspect of this study. The water-to-solid ratio denotes the proportion of water used in the carbonation process relative to the quantity of waste concrete powder. The changes in the WSR have the potential to influence $CO_2$ absorption capacity, potentially leading to enhancement due to improved interaction between $CO_2$ and the WCP. Additionally, at the beginning of the process, with a decrease in WSR or with an increase in the solid–liquid ratio, there is a corresponding elevation in the amount of $CO_2$ uptake. This implies a greater availability of calcium (Ca) to engage in $CO_2$ capture and the subsequent formation of calcium carbonate ($CaCO_3$). Additionally, the $CO_2$ uptake efficiency (measured as g-$CO_2$/g-concrete fines) remains relatively consistent, showing a slight increase with higher solid–liquid ratios, as displayed in Table 1. Furthermore, water distribution within the material plays a role in the uniformity of carbonation, and variations in the ratio can also lead to changes in physical properties. Therefore, determining the optimal WSR becomes crucial, similar to CT, in order to attain effective $CO_2$ capture.

### *3.1. Modeling Phase*

The ANFIS framework was constructed based on a dataset of 23 experiments, with the dataset divided into two groups for training and testing purposes. The first group, comprising 18 points, was used for training the model, and the remaining points were designated for testing the model's performance. The hybrid training method integrated least squares estimation in the forward path and utilized backpropagation for the backward direction to achieve an effective training process. A set of 10 fuzzy rules for the system was derived using the subtractive clustering method. The model was trained iteratively until a reduced RMSE was achieved. Table 2 presents the statistical metrics obtained from the ANFIS model.

**Table 2.** Statistical analysis of ANFIS model of $CO_2$ uptake.

| RMSE | | | Coefficient of Determination | | |
|---|---|---|---|---|---|
| **Training** | **Testing** | **All** | **Training** | **Testing** | **All** |
| $3.3124 \times 10^{-6}$ | 0.022 | 0.0102 | 1.0 | 0.9994 | 0.9999 |

The ANFIS model for $CO_2$ uptake exhibited RMSE values of $3.3124 \times 10^{-6}$ and 0.022 for the training and testing datasets, respectively, as displayed in Table 2. The R-Square for the training and testing stages are 1.0 and 0.9994, respectively, as presented in Table 2. Comparing these results with ANOVA [23], the R-Square has increased by approximately 19% from 0.84 using ANOVA to 0.9999 using ANFIS. Additionally, the RMSE has significantly decreased from 1.96 using ANOVA to 0.0102 using ANFIS, indicating the effectiveness of the ANFIS modeling phase. Figure 3 demonstrates the architecture of the ANFIS model with two inputs and one output, while Figure 4 displays the general contours of the Gaussian-form MFs.

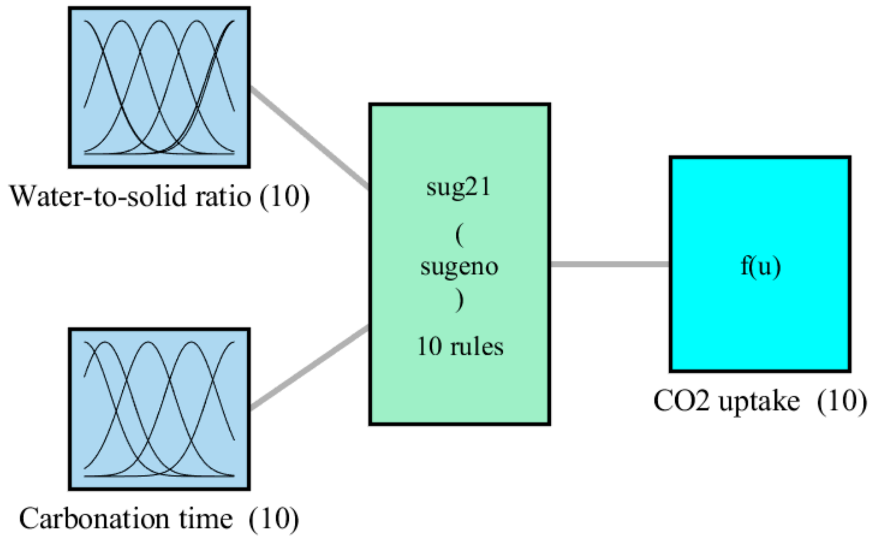


**Figure 3.** Configuration of ANFIS framework $CO_2$ uptake.

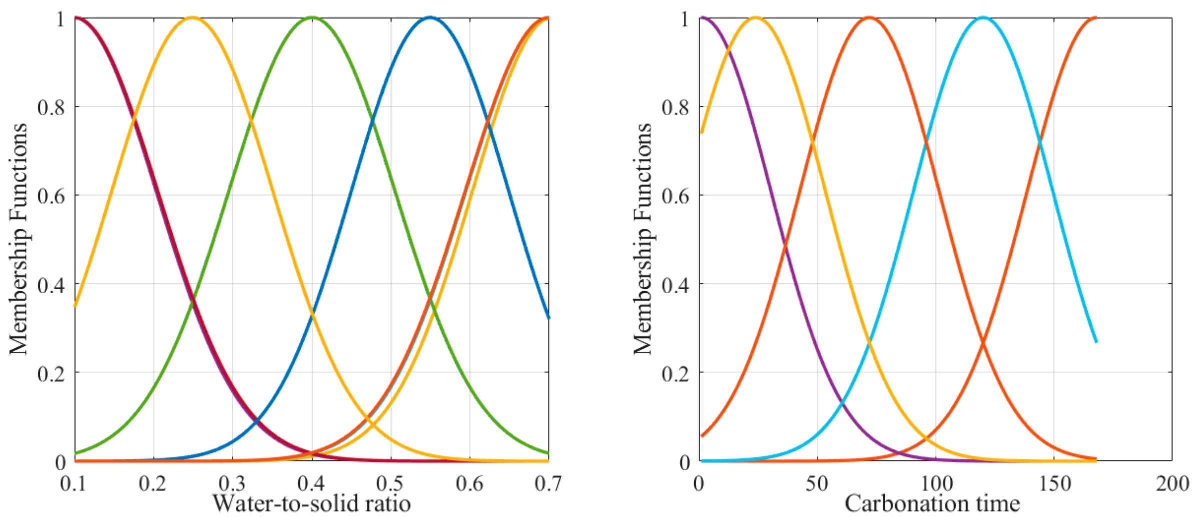


**Figure 4.** Input MFs of ANFIS framework of $CO_2$ uptake. Each color represents fuzzy membership function.

Figure 5 presents a spatial representation from a 3-D perspective, illustrating the contours of the input–output function for each combination of inputs. The color gradient ranges from dark red, representing the highest output value of $CO_2$ uptake, to blue, indicating the lowest. The figure demonstrates the integration of ANFIS and MPA, highlighting the accomplishment of a remarkable $CO_2$ uptake rate of 3.86%. This optimization is achieved through the identification of the optimal carbonation time (CT) of 54.3 h and the selection of a suitable water-to-solid ratio (WSR) of 0.327.

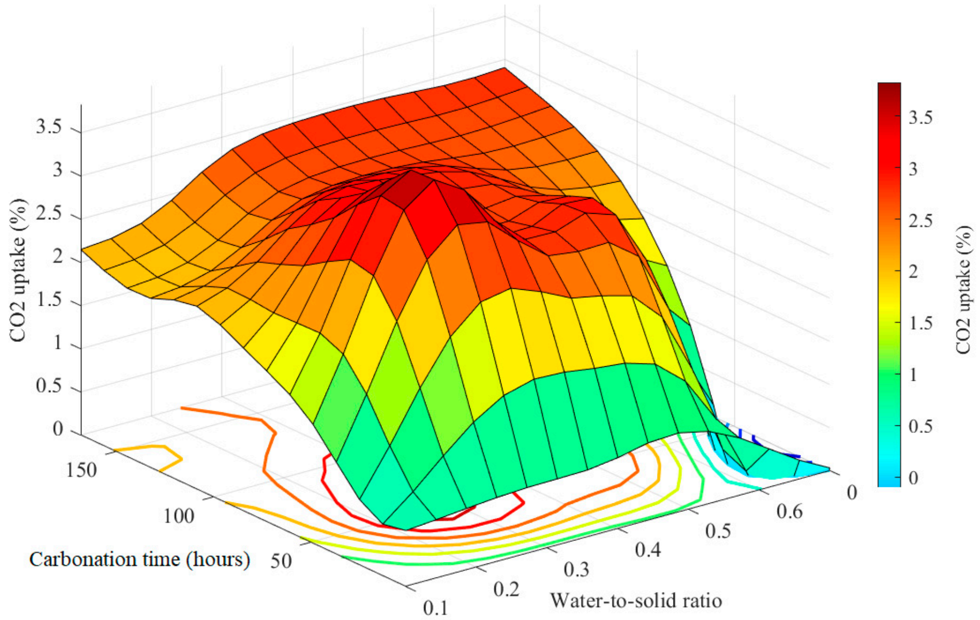


**Figure 5.** Three-dimensional plot of controlling parameters.

Figure 6 displays the comparison between the predicted and measured data of the ANFIS model for $CO_2$ uptake. The plot demonstrates a strong alignment between the estimated and measured values. This alignment between the estimated and measured values is particularly robust, indicating a high level of accuracy and reliability in the ANFIS model's predictive capabilities; furthermore, Figure 7 exhibits the prediction results for both the training and testing phases, depicting a close approximation to the line of 100% accuracy.

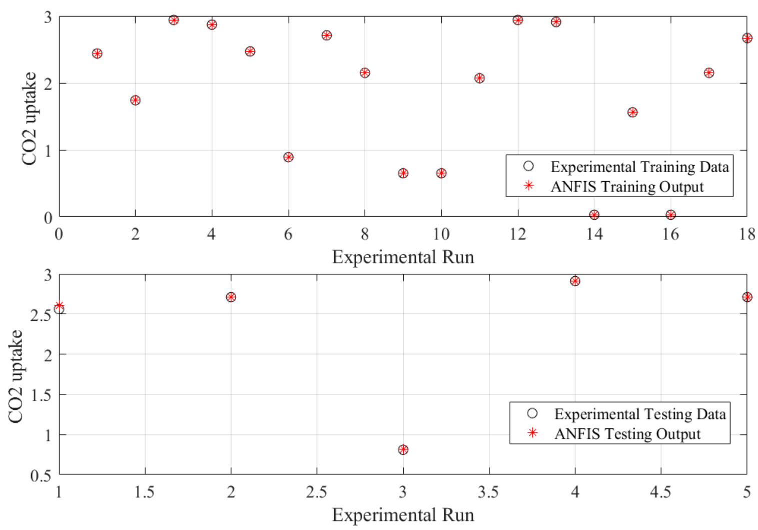


**Figure 6.** Predicted vs. experimental output of ANFIS $CO_2$ uptake model.

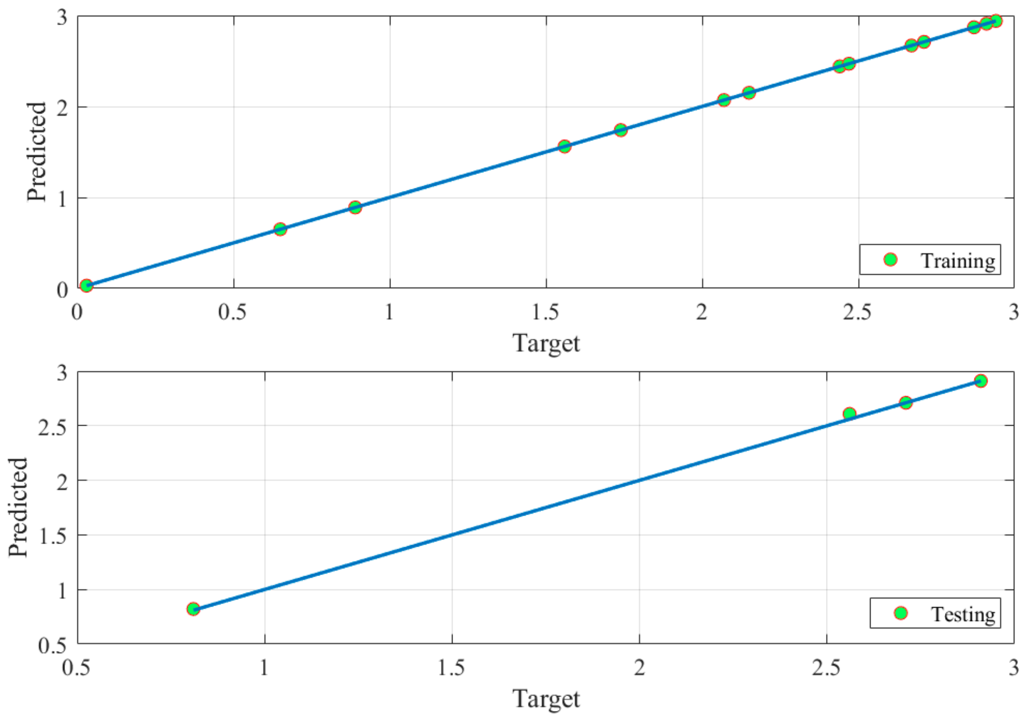


**Figure 7.** Prediction accuracy of ANFIS $CO_2$ uptake model.

Table 3 presents the validation results of the ANFIS model for $CO_2$ uptake in comparison to ANOVA. The absolute error values for $CO_2$ uptake are 0.25 and 0.14, respectively, when compared to the experimental data for ANOVA and ANFIS. The ANFIS model exhibits a 44% reduction in absolute error for $CO_2$ uptake compared to ANOVA. Furthermore, the percentage error values are 8.83% and 4.95% for ANOVA and ANFIS, respectively. These findings highlight the superior performance of the ANFIS model when compared to the ANOVA model.

**Table 3.** Validation of ANFIS model of $CO_2$ uptake.

| | WSR | CT | $CO_2$ Uptake (%) | AE | % Error |
|---|---|---|---|---|---|
| Experimental [23] | 0.32 | 72 h | 2.83 | - | - |
| ANOVA [23] | 0.32 | 72 h | 5.58 | 0.25 | 8.83 |
| ANFIS and MPA | 0.32 | 72 h | 2.97 | 0.14 | 4.95 |

### 3.2. Optimization Phase

In this section, the objective was to determine the optimal values of the water-to-solid ratio (WSR) and carbonation time (CT) that would result in a high $CO_2$ uptake percentage. To achieve this, the Marine Predators Algorithm (MPA) was utilized in combination with reliable ANFIS models of $CO_2$ uptake. In the process of optimization, the two parameters CT and WSR are utilized as decision variables, aiming to maximize the $CO_2$ uptake, which functions as the objective function. The optimized results obtained using the experimental, RSM, and recommended methods are displayed in Table 4. The integration of ANFIS and MPA led to a significant increase in the $CO_2$ uptake percentage by approximately 30% compared to the experimental data and RSM. The optimal values under these conditions were found to be 0.27 for the WSR and 54.3 h for the CT. Figure 8 provides a visual representation of the convergence process of particles concerning three key aspects: the objective function, WSR, and CT. The figure offers a clear trajectory of each particle's iterative approach toward the optimal values of these parameters. It can be observed that all particles converged to the optimal values within 20 iterations. This concise and efficient convergence underscores the efficacy of the method employed, instilling confidence in the precision and reliability of the obtained optimal parameter values.

**Table 4.** Optimized results using experimental, RSM, and proposed methods.

| | WSR | CT (h) | $CO_2$ Uptake (%) |
|---|---|---|---|
| Experimental [4] | 0.4 | 168 | 2.94 |
| RSM [4] | 0.4 | 90 | 2.8 |
| ANFIS and MPA | 0.27 | 54.3 | 3.86 |

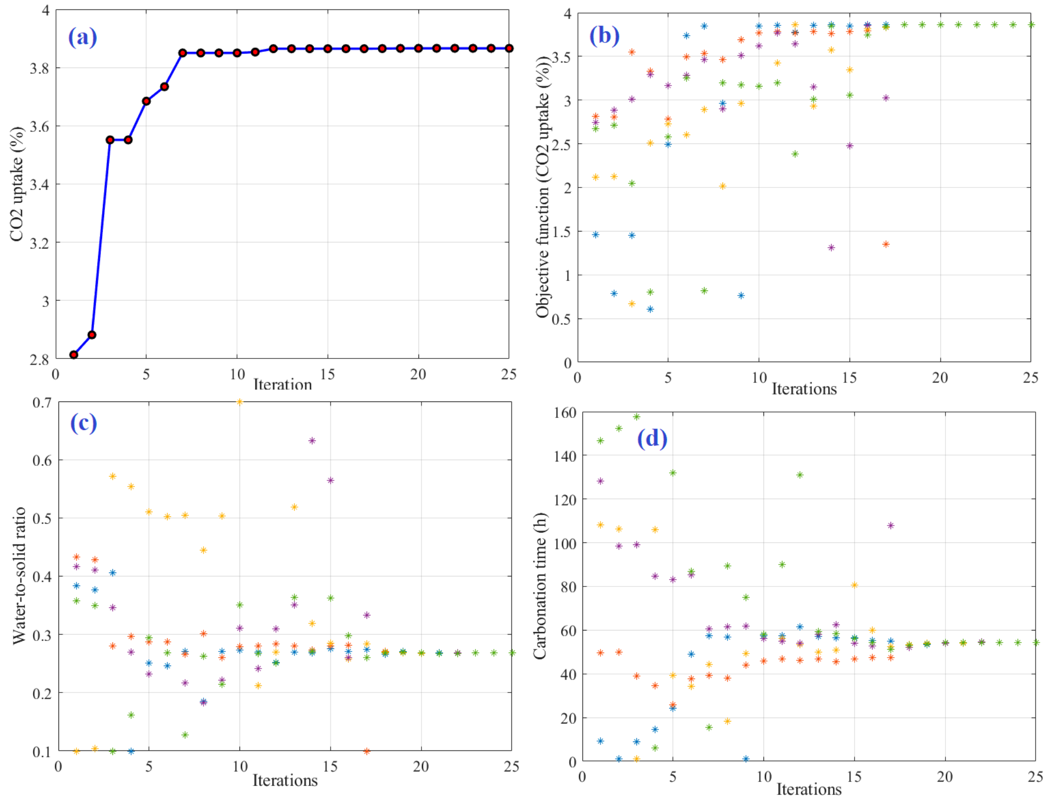


**Figure 8.** The phenomenon of particles converging while performing parameter identification (**a**) $CO_2$ uptake, (**b**) objective function, (**c**) WSR, and (**d**) CT.

The Particle Swarm Optimization (PSO), Genetic Algorithm (GA), Harris Hawks Optimization (HHO), and Cuckoo Search (CS) outcomes are compared to validate the MPA suppository. To ensure consistent outcomes, each optimizer is executed 30 times, and a comprehensive statistical analysis is performed. Table 5 and Figure 9 present the detailed results of 30 runs utilizing different optimizers. Statistical indicators such as the highest value, lowest value, average value, and standard deviation are computed and presented in Table 6. The average values of the cost function (based on the ANFIS model of $CO_2$ uptake) range from 3.762 to 3.857. The MPA achieved the highest average value (3.857), followed by PSO (3.836), and then GA (3.762) with the lowest average value. The standard deviation values range from 0.002 to 0.184, where MPA demonstrates the best standard deviation (STD) value of 0.002, followed by HHO (0.055), and CS (0.184). These results highlight the effectiveness of MPA in identifying optimal values that lead to the highest $CO_2$ uptake.

**Table 5.** Details of 30 runs using different optimizers.

| No. | PSO | MPA | HHO | CS | GA | No. | PSO | MPA | HHO | CS | GA |
|---|---|---|---|---|---|---|---|---|---|---|---|
| 1 | 3.864 | 3.866 | 3.834 | 3.865 | 3.845 | 16 | 3.866 | 3.866 | 3.748 | 3.866 | 3.821 |
| 2 | 3.866 | 3.866 | 3.833 | 3.866 | 3.752 | 17 | 3.866 | 3.866 | 3.79 | 3.861 | 3.798 |
| 3 | 3.865 | 3.866 | 3.862 | 3.866 | 3.865 | 18 | 3.863 | 3.86 | 3.857 | 3.866 | 3.632 |
| 4 | 3.864 | 3.866 | 3.851 | 3.866 | 3.835 | 19 | 3.866 | 3.866 | 3.797 | 3.866 | 3.521 |
| 5 | 3.865 | 3.866 | 3.675 | 3.866 | 3.803 | 20 | 3.865 | 3.866 | 3.855 | 3.866 | 3.84 |
| 6 | 3.865 | 3.865 | 3.866 | 3.866 | 3.863 | 21 | 3.865 | 3.866 | 3.862 | 3.865 | 3.849 |
| 7 | 3.866 | 3.866 | 3.81 | 3.863 | 3.851 | 22 | 3.864 | 3.866 | 3.829 | 2.987 | 3.815 |
| 8 | 3.866 | 3.866 | 3.857 | 3.863 | 3.858 | 23 | 3.864 | 3.866 | 3.866 | 3.855 | 3.862 |
| 9 | 3.866 | 3.866 | 3.866 | 3.865 | 3.865 | 24 | 3.866 | 3.866 | 3.86 | 3.866 | 3.844 |
| 10 | 3.863 | 3.866 | 3.863 | 3.865 | 3.843 | 25 | 3.866 | 3.866 | 3.86 | 3.814 | 3.772 |
| 11 | 3.866 | 3.866 | 3.85 | 3.372 | 3.864 | 26 | 3.866 | 3.857 | 3.862 | 3.866 | 3.801 |
| 12 | 3.866 | 3.866 | 3.659 | 3.86 | 3.653 | 27 | 3.865 | 3.866 | 3.79 | 3.866 | 3.86 |
| 13 | 3.866 | 3.866 | 3.863 | 3.748 | 3.527 | 28 | 3.864 | 3.866 | 3.864 | 3.866 | 3.848 |
| 14 | 2.993 | 3.864 | 3.846 | 3.866 | 3.467 | 29 | 3.864 | 3.866 | 3.815 | 3.866 | 3.836 |
| 15 | 3.864 | 3.866 | 3.842 | 3.552 | 3.7 | 30 | 3.866 | 3.866 | 3.72 | 3.865 | 3.167 |

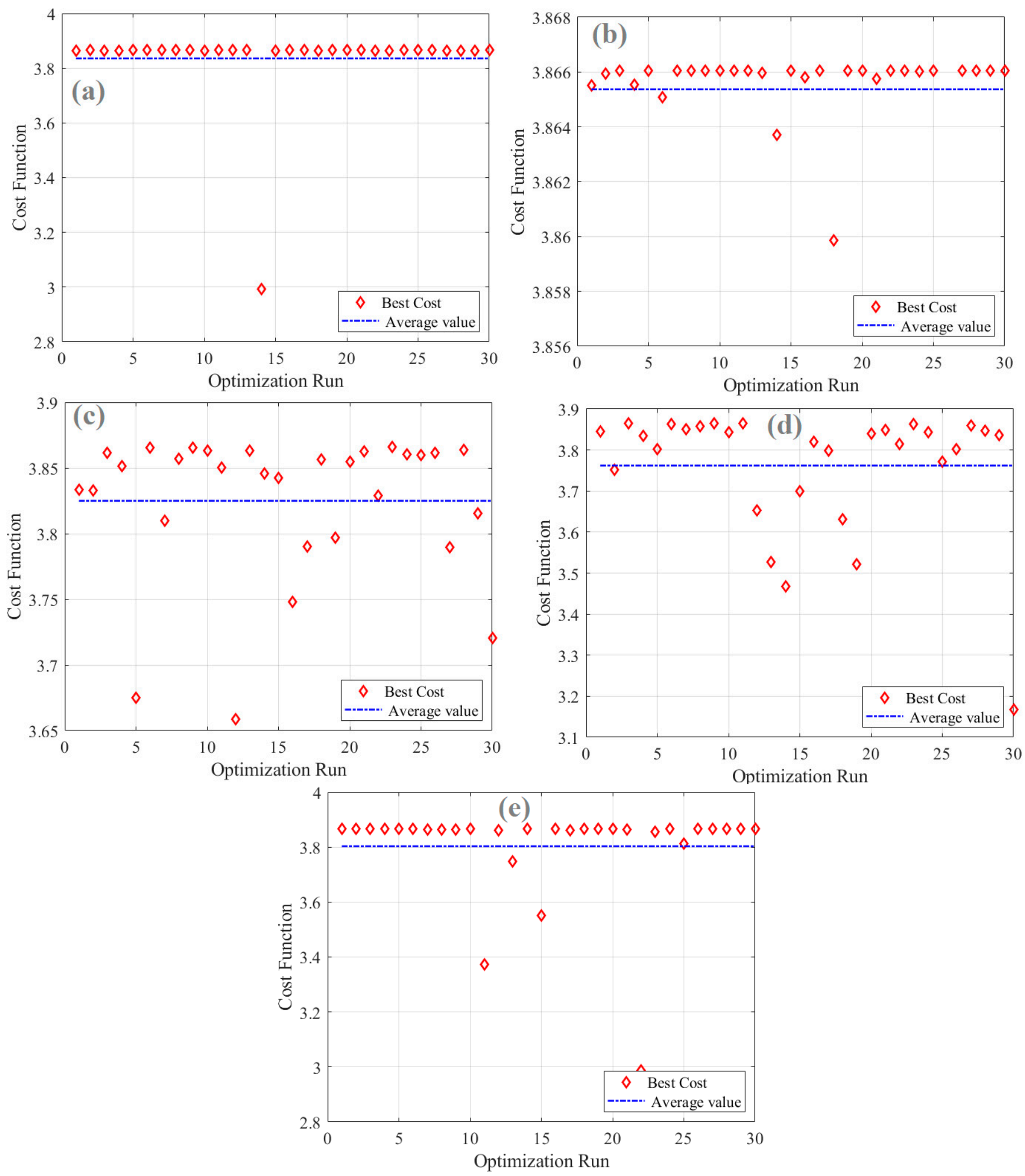


**Figure 9.** Details of 30 runs: (**a**) PSO, (**b**) MPA, (**c**) HHO, (**d**) GA, and (**e**) CS.

**Table 6.** Statistical evaluation for considered optimizers.

| | PSO | MPA | HHO | CS | GA |
|---|---|---|---|---|---|
| Best | 3.866 | 3.866 | 3.866 | 3.866 | 3.865 |
| Worst | 2.993 | 3.857 | 3.659 | 2.987 | 3.167 |
| Mean | 3.836 | 3.865 | 3.825 | 3.803 | 3.762 |
| STD | 0.157 | 0.002 | 0.055 | 0.184 | 0.156 |

## 4. Conclusions

Exploring the enhancement of $CO_2$ uptake from waste concrete powder yields a range of advantages, including minimizing environmental impact by reducing building waste accumulation, fostering resource efficiency through waste utilization, and promoting sustainable construction practices. The percentage value of $CO_2$ uptake of WCP from a recycling plant for building and demolition debris is influenced by two primary factors: the WSR and the CT. The objective of this study is to identify the optimal values for the WSR and CT in order to maximize $CO_2$ uptake. The integration of artificial intelligence, specifically the Adaptive ANFIS model and the Marine Predators Algorithm (MPA), was employed for the modeling and parameter identification processes. During the modeling phase, the ANFIS model demonstrated excellent performance with low RMSE values of $3.3124 \times 10^{-6}$ for the training data set and 0.022 for the testing data set. The coefficients of determination were also high, with values of 1.0 for training and 0.9994 for testing. Compared with the traditional ANOVA method, the ANFIS model achieved a significant improvement in the coefficient of determination from 0.84 to 0.9999, indicating a 19% increase. Additionally, the RMSE decreased from 1.96 to 0.0102, indicating the effectiveness of the ANFIS modeling phase. The integration of ANFIS and MPA led to a substantial increase in the percentage value of $CO_2$ uptake, improving it by approximately 30% in comparison to the experimental results and the RSM. Under these optimized conditions, the best values for the WSR and CT were found to be 0.27 and 54.3 h, respectively. Overall, this study demonstrates the effectiveness of the integrated ANFIS and MPA approach in improving the $CO_2$ uptake percentage for waste concrete powder. The findings provide valuable insights for optimizing the WSR and CT in the recycling process, leading to more sustainable and environmentally friendly practices in the construction industry.

**Author Contributions:** Conceptualization, H.R. and A.A.; Methodology, H.R., A.A. and R.M.G.; Software, H.R. and R.M.G.; Validation, R.M.G.; Formal analysis, H.R., A.A., R.M.G. and S.A.; Investigation, A.A. and S.A.; Resources, S.A.; Writing—original draft, H.R., A.A., R.M.G. and S.A.; Writing—review & editing, H.R. and A.A.; Visualization, A.A. and S.A. All authors have read and agreed to the published version of the manuscript.

**Funding:** Princess Nourah bint Abdulrahman University Researchers Supporting Project number (PNURSP2023R138), Princess Nourah bint Abdulrahman University, Riyadh, Saudi Arabia.

**Data Availability Statement:** Not applicable.

**Acknowledgments:** The authors express their gratitude to the Middle East University in Amman, Jordan for providing financial support to cover the publication fees associated with this research article.

**Conflicts of Interest:** The authors declare no conflict of interest.

## References

1. Kaliyavaradhan, S.K.; Ling, T.-C. Potential of $CO_2$ Sequestration through Construction and Demolition (C&D) Waste—An Overview. *J. $CO_2$ Util.* **2017**, *20*, 234–242.
2. Xuan, D.; Zhan, B.; Poon, C.S.; Zheng, W. Carbon Dioxide Sequestration of Concrete Slurry Waste and Its Valorisation in Construction Products. *Constr. Build. Mater.* **2016**, *113*, 664–672. [CrossRef]
3. Madejski, P.; Chmiel, K.; Subramanian, N.; Kuś, T. Methods and Techniques for $CO_2$ Capture: Review of Potential Solutions and Applications in Modern Energy Technologies. *Energies* **2022**, *15*, 887. [CrossRef]
4. Odunlami, O.A.; Vershima, D.A.; Oladimeji, T.E.; Nkongho, S.; Ogunlade, S.K.; Fakinle, B.S. Advanced Techniques for the Capturing and Separation of $CO_2$–a Review. *Results Eng.* **2022**, *15*, 100512. [CrossRef]

5. Chen, L.; Msigwa, G.; Yang, M.; Osman, A.I.; Fawzy, S.; Rooney, D.W.; Yap, P.-S. Strategies to Achieve a Carbon Neutral Society: A Review. *Environ. Chem. Lett.* **2022**, *20*, 2277–2310. [CrossRef]
6. Shahbazi, A.; Nasab, B.R. Carbon Capture and Storage (CCS) and Its Impacts on Climate Change and Global Warming. *J. Pet. Environ. Biotechnol.* **2016**, *7*, 1000291. [CrossRef]
7. Fang, W.; Guangzhi, L.; Chunmei, S.U.; Feng, W.; Jianguo, M.A.; Yongzhi, Y. Carbon Emission Reduction Accounting Method for a CCUS-EOR Project. *Pet. Explor. Dev.* **2023**, *50*, 989–1000.
8. Thakur, I.S.; Kumar, M.; Varjani, S.J.; Wu, Y.; Gnansounou, E.; Ravindran, S. Sequestration and Utilization of Carbon Dioxide by Chemical and Biological Methods for Biofuels and Biomaterials by Chemoautotrophs: Opportunities and Challenges. *Bioresour. Technol.* **2018**, *256*, 478–490. [CrossRef]
9. Desport, L.; Selosse, S. An Overview of $CO_2$ Capture and Utilization in Energy Models. *Resour. Conserv. Recycl.* **2022**, *180*, 106150. [CrossRef]
10. Guduru, R.K.; Gupta, A.A.; Dixit, U. Chapter 13—Biological Processes for $CO_2$ Capture. In *Emerging Carbon Capture Technologies*; Elsevier: Amsterdam, The Netherlands, 2022; pp. 371–400.
11. Foteinis, S.; Campbell, J.S.; Renforth, P. Life Cycle Assessment of Coastal Enhanced Weathering for Carbon Dioxide Removal from Air. *Environ. Sci. Technol.* **2023**, *57*, 6169–6178. [CrossRef]
12. Erans, M.; Sanz-Pérez, E.S.; Hanak, D.P.; Clulow, Z.; Reiner, D.M.; Mutch, G.A. Direct Air Capture: Process Technology, Techno-Economic and Socio-Political Challenges. *Energy Environ. Sci.* **2022**, *15*, 1360–1405. [CrossRef]
13. Alamayreh, M.I.; Alahmer, A.; Younes, M.B.; Bazlamit, S.M. Pre-Cooling Concrete System in Massive Concrete Production: Energy Analysis and Refrigerant Replacement. *Energies* **2022**, *15*, 1129. [CrossRef]
14. Sáez, P.V.; Osmani, M. A Diagnosis of Construction and Demolition Waste Generation and Recovery Practice in the European Union. *J. Clean. Prod.* **2019**, *241*, 118400. [CrossRef]
15. Gálvez-Martos, J.-L.; Styles, D.; Schoenberger, H.; Zeschmar-Lahl, B. Construction and Demolition Waste Best Management Practice in Europe. *Resour. Conserv. Recycl.* **2018**, *136*, 166–178. [CrossRef]
16. Kazemian, M.; Shafei, B. Carbon Sequestration and Storage in Concrete: A State-of-the-Art Review of Compositions, Methods, and Developments. *J. $CO_2$ Util.* **2023**, *70*, 102443. [CrossRef]
17. Amran, M.; Makul, N.; Fediuk, R.; Lee, Y.H.; Vatin, N.I.; Lee, Y.Y.; Mohammed, K. Global Carbon Recoverability Experiences from the Cement Industry. *Case Stud. Constr. Mater.* **2022**, *17*, e01439. [CrossRef]
18. Lim, M.; Han, G.-C.; Ahn, J.-W.; You, K.-S. Environmental Remediation and Conversion of Carbon Dioxide ($CO_2$) into Useful Green Products by Accelerated Carbonation Technology. *Int. J. Environ. Res. Public Health* **2010**, *7*, 203–228. [CrossRef] [PubMed]
19. Ueno, A.; Kawai, K.; Kobayashi, K.; Tanaka, S. Evaluation of Visual Methods for $CO_2$ Uptake by Demolished Concrete: Research Activities by JSCE Subcommittee 219. *Constr. Build. Mater.* **2014**, *67*, 393–398. [CrossRef]
20. Kaliyavaradhan, S.K.; Ling, T.-C.; Mo, K.H. Valorization of Waste Powders from Cement-Concrete Life Cycle: A Pathway to Circular Future. *J. Clean. Prod.* **2020**, *268*, 122358. [CrossRef]
21. Olajire, A.A. A Review of Mineral Carbonation Technology in Sequestration of $CO_2$. *J. Pet. Sci. Eng.* **2013**, *109*, 364–392. [CrossRef]
22. Deng, S.; Ren, P.; Jiang, Y.; Shao, X.; Ling, T.-C. Use of $CO_2$-Active BOFS Binder in the Production of Artificial Aggregates with Waste Concrete Powder. *Resour. Conserv. Recycl.* **2022**, *182*, 106332. [CrossRef]
23. Kaliyavaradhan, S.K.; Li, L.; Ling, T.-C. Response Surface Methodology for the Optimization of $CO_2$ Uptake Using Waste Concrete Powder. *Constr. Build. Mater.* **2022**, *340*, 127758. [CrossRef]
24. Bu, C.; Tan, B.; Wu, Q.; Qiao, Y.; Sun, Y.; Yu, L.; Yang, Q. Activation Method and Reuse of Waste Concrete Powder—A Review. *Sustainability* **2023**, *15*, 5451. [CrossRef]
25. Possan, E.; Felix, E.F.; Thomaz, W.A. $CO_2$ Uptake by Carbonation of Concrete during Life Cycle of Building Structures. *J. Build. Pathol. Rehabil.* **2016**, *1*, 7. [CrossRef]
26. Kaliyavaradhan, S.K.; Ling, T.-C.; Mo, K.H. $CO_2$ Sequestration of Fresh Concrete Slurry Waste: Optimization of $CO_2$ Uptake and Feasible Use as a Potential Cement Binder. *J. $CO_2$ Util.* **2020**, *42*, 101330. [CrossRef]
27. Pan, S.-Y.; Chen, Y.-H.; Fan, L.-S.; Kim, H.; Gao, X.; Ling, T.-C.; Chiang, P.-C.; Pei, S.-L.; Gu, G. $CO_2$ Mineralization and Utilization by Alkaline Solid Wastes for Potential Carbon Reduction. *Nat. Sustain.* **2020**, *3*, 399–405. [CrossRef]
28. Haug, T.A.; Kleiv, R.A.; Munz, I.A. Investigating Dissolution of Mechanically Activated Olivine for Carbonation Purposes. *Appl. Geochem.* **2010**, *25*, 1547–1563. [CrossRef]
29. Chang, E.-E.; Pan, S.-Y.; Chen, Y.-H.; Chu, H.-W.; Wang, C.-F.; Chiang, P.-C. $CO_2$ Sequestration by Carbonation of Steelmaking Slags in an Autoclave Reactor. *J. Hazard. Mater.* **2011**, *195*, 107–114. [CrossRef]
30. Pan, S.-Y.; Chang, E.E.; Chiang, P.-C. $CO_2$ Capture by Accelerated Carbonation of Alkaline Wastes: A Review on Its Principles and Applications. *Aerosol Air Qual. Res.* **2012**, *12*, 770–791. [CrossRef]
31. Xuan, D.; Zhan, B.; Poon, C.S.; Zheng, W. Innovative Reuse of Concrete Slurry Waste from Ready-Mixed Concrete Plants in Construction Products. *J. Hazard. Mater.* **2016**, *312*, 65–72. [CrossRef]
32. Alahmer, A.; Alahmer, H.; Handam, A.; Rezk, H. Environmental Assessment of a Diesel Engine Fueled with Various Biodiesel Blends: Polynomial Regression and Grey Wolf Optimization. *Sustainability* **2022**, *14*, 1367. [CrossRef]
33. Alahmer, H.; Alahmer, A.; Alkhazaleh, R.; Al-Amayreh, M.I. Modeling, Polynomial Regression, and Artificial Bee Colony Optimization of SI Engine Performance Improvement Powered by Acetone–Gasoline Fuel Blends. *Energy Rep.* **2023**, *9*, 55–64. [CrossRef]

34. Ghoniem, R.M.; Alahmer, A.; Rezk, H.; As'ad, S. Optimal Design and Sizing of Hybrid Photovoltaic/Fuel Cell Electrical Power System. *Sustainability* **2023**, *15*, 12026. [CrossRef]
35. Jang, J.-S. ANFIS: Adaptive-Network-Based Fuzzy Inference System. *IEEE Trans. Syst. Man. Cybern.* **1993**, *23*, 665–685. [CrossRef]
36. Lin, Y.-H.; Chang, W.-J.; Ku, C.-C. Solving the Formation and Containment Control Problem of Nonlinear Multi-Boiler Systems Based on Interval Type-2 Takagi–Sugeno Fuzzy Models. *Processes* **2022**, *10*, 1216. [CrossRef]
37. Tiruneh, G.G.; Fayek, A.R.; Sumati, V. Neuro-Fuzzy Systems in Construction Engineering and Management Research. *Autom. Constr.* **2020**, *119*, 103348. [CrossRef]
38. Faramarzi, A.; Heidarinejad, M.; Mirjalili, S.; Gandomi, A.H. Marine Predators Algorithm: A Nature-Inspired Metaheuristic. *Expert Syst. Appl.* **2020**, *152*, 113377. [CrossRef]
39. Zhang, J.; Xu, Y. Training Feedforward Neural Networks Using an Enhanced Marine Predators Algorithm. *Processes* **2023**, *11*, 924. [CrossRef]